Updated plots of the “new version” of the manuscript

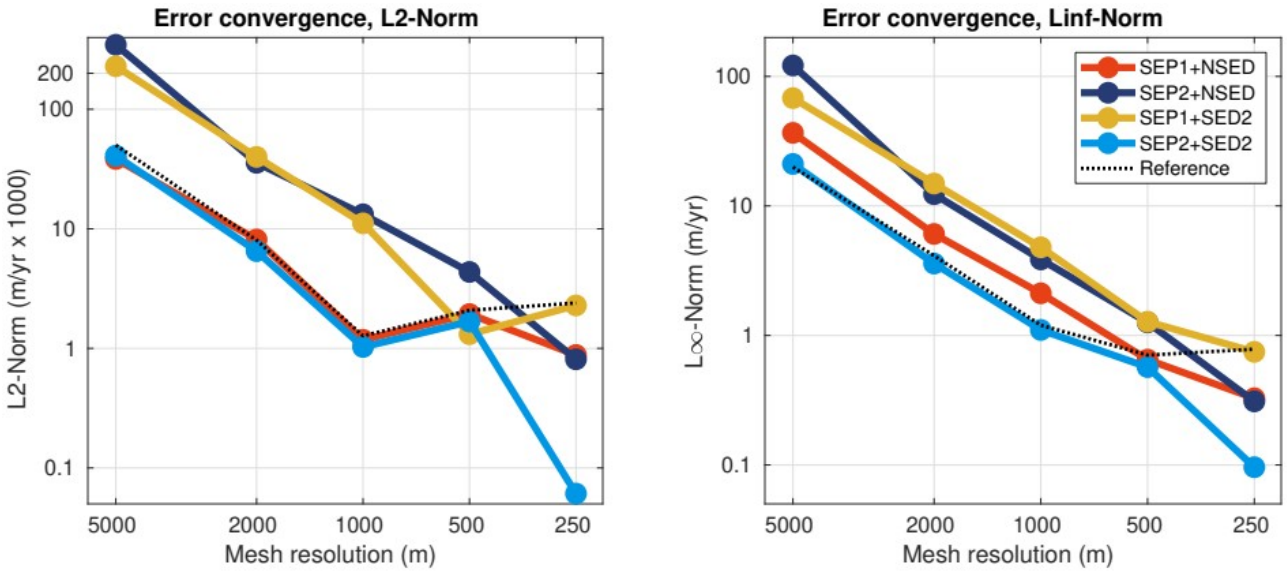

Figure 3. Error convergence of the ice speed for the diagnostic analysis in L2-norm (left panel) and Linf-norm (right panel). All sets of sub-element parameterizations are shown: SEP1+NSED, SEP2+NSED, SEP1+SED2, and SEP2+SED2. The error convergence from structured-conforming-mesh-based models is also shown (Reference, dotted line).

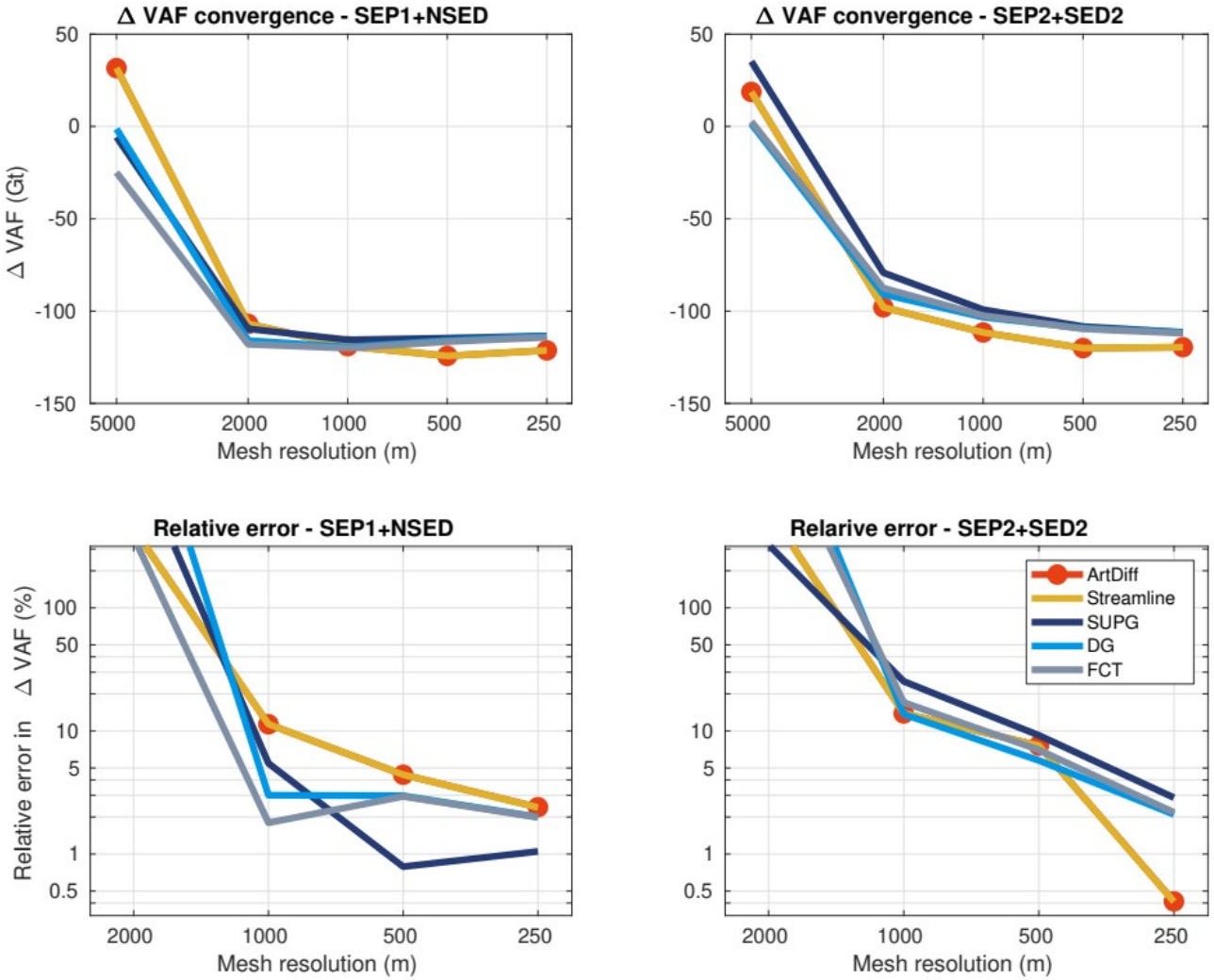

Figure 6. No external forcing experiment: convergence of volume above floatation change (DeltaVAF) at the end of the experiment (t=100 yr) for different stabilization schemes (see legend). Two sets of parameterizations are employed: SEP1+NSED (left panels) and SEP2+SED2 (right panels). The relative errors are computed using Eq. 45.

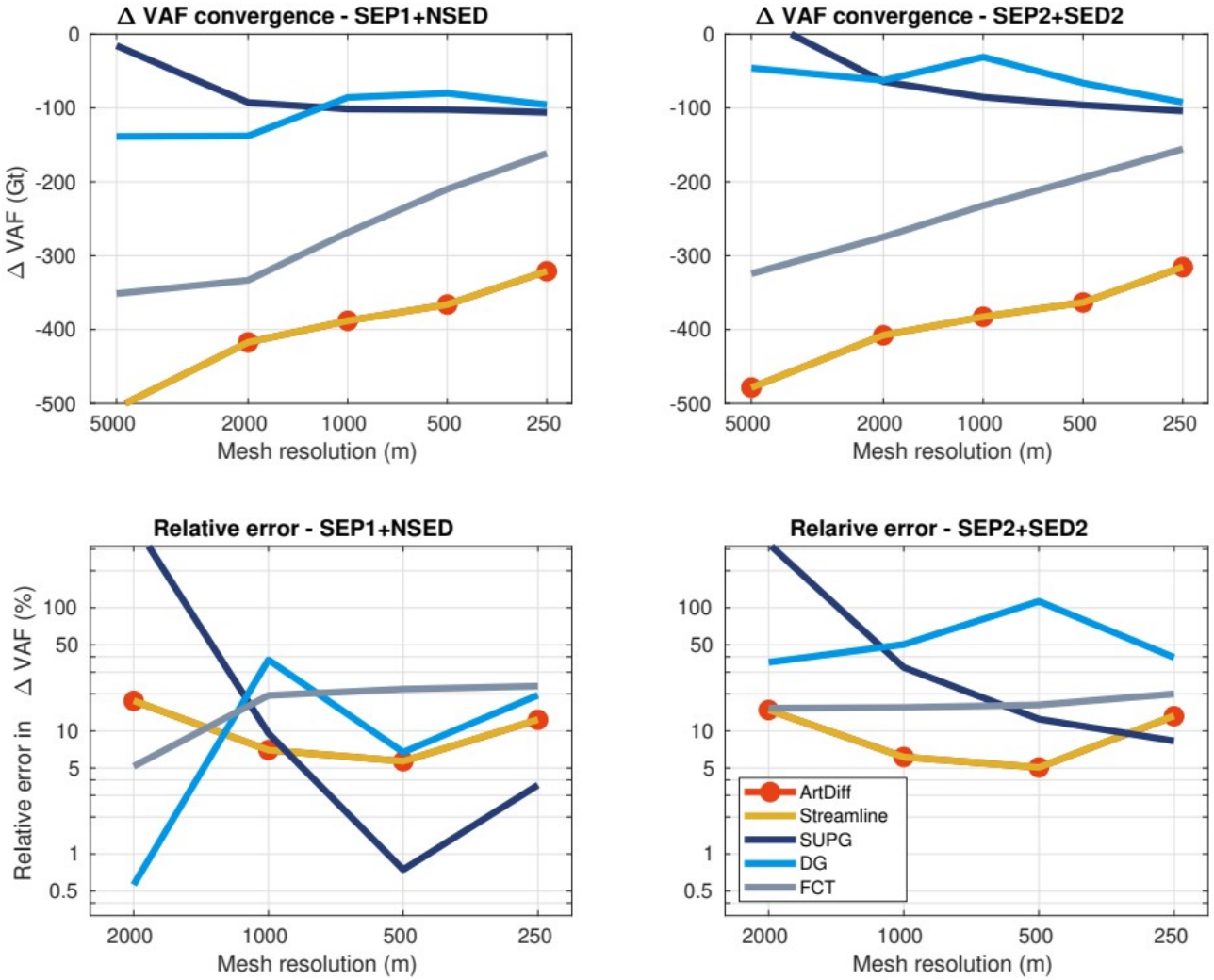

Figure 8. Basal melt experiment (no melt on partly floating elements): convergence of volume above floatation change (DeltaVAF) at the end of the experiment (t=100 yr) for different stabilization schemes (see legend). Two sets of sub-element parameterizations are employed: SEP1+NSED (left panels) and SEP2+SED2 (right panels). The relative errors are computed using Eq. 45.

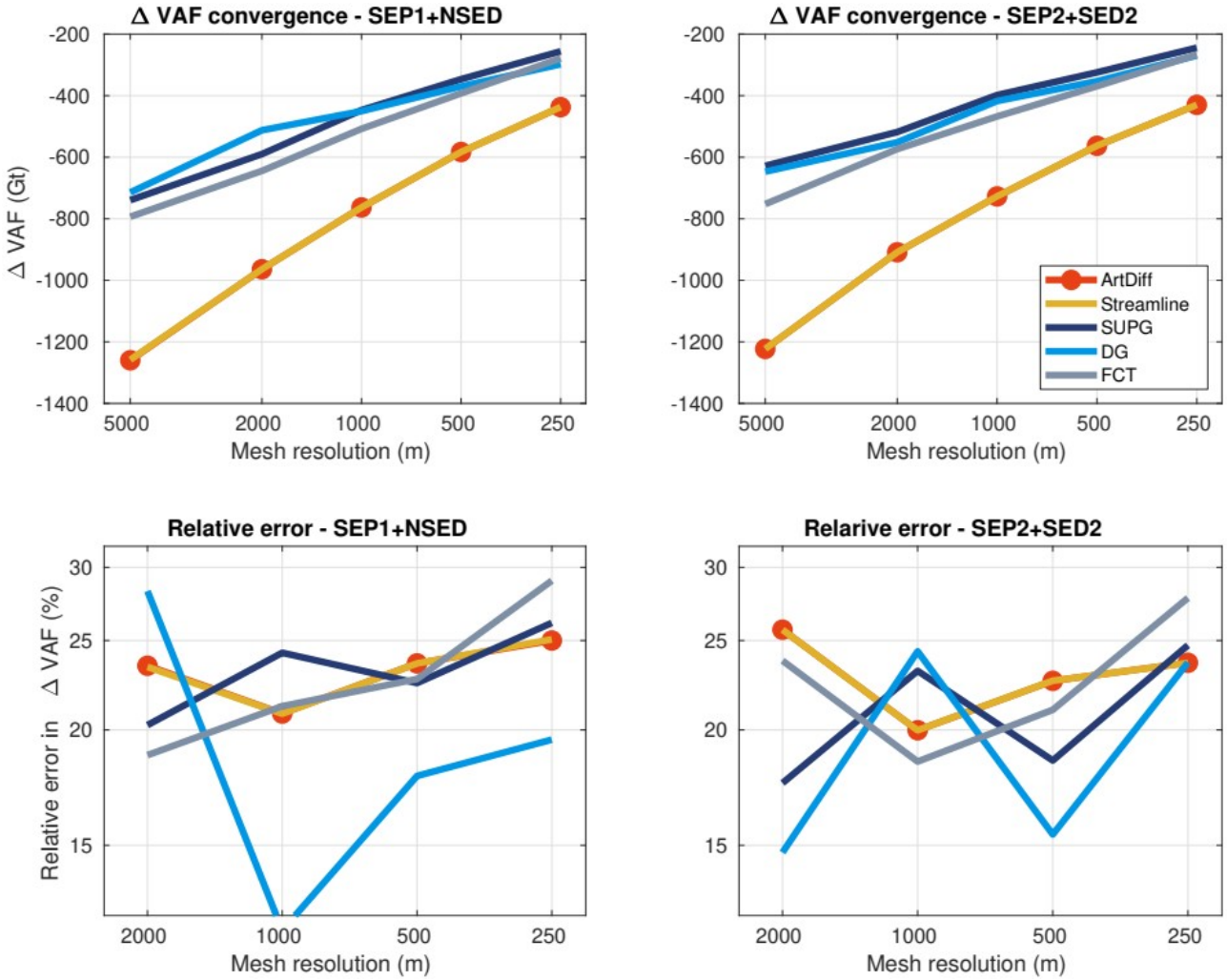

Figure 11. Basal melt experiment (melt on partly floating elements): convergence of volume above floatation change (DeltaVAF) at the end of the experiment (t=100 yr) for different stabilization schemes (see legend). Two sets of sub-element parameterizations are employed: SEP1+NSED (left panels) and SEP2+SED2 (right panels). The relative errors are computed using Eq. 45.

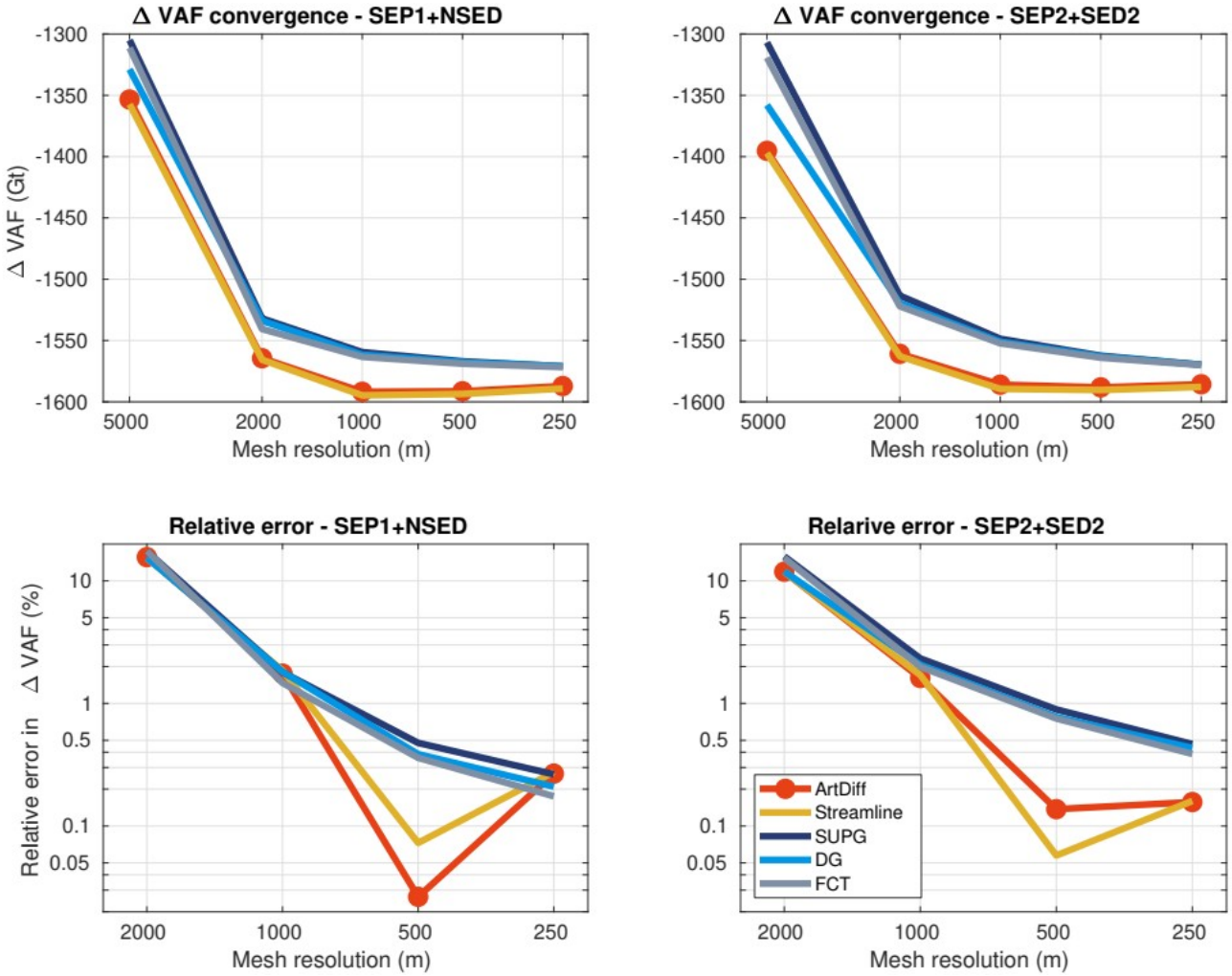

Figure 13. Basal friction perturbation experiment: convergence of volume above floatation change (DeltaVAF) at the end of the experiment (t=100 yr) for different stabilization schemes (see legend). Two sets of sub-element parameterizations are employed: SEP1+NSED (left panels) and SEP2+SED2 (right panels). The relative errors are computed using Eq. 45.

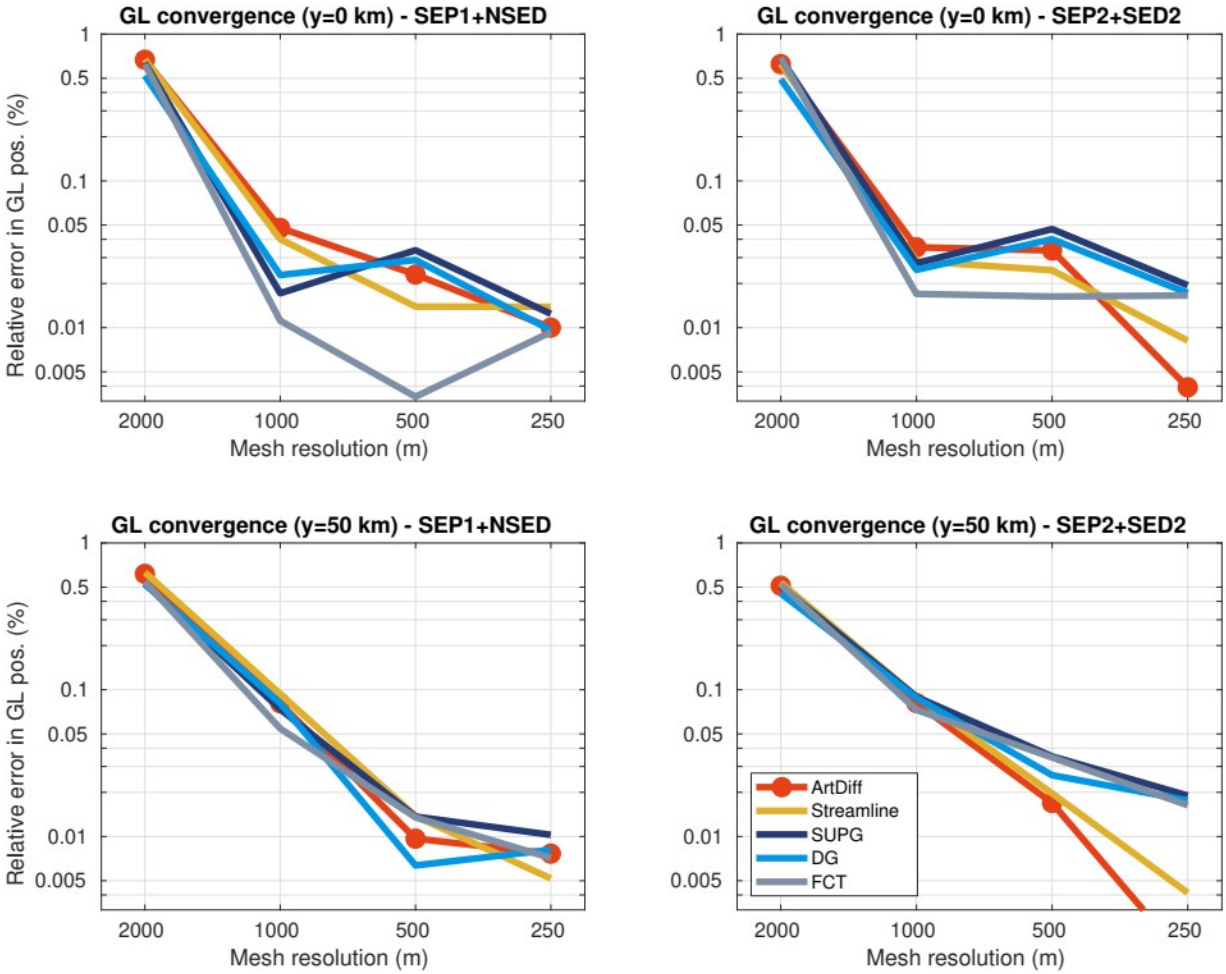

Figure 15. Basal friction perturbation experiment: convergence of grounding line positions (relative errors) at the end of the experiment (t=100 yr), for y=0 (top panels) and y=50 km (bottom panels), and for different stabilization schemes (see legend). Two sets of sub-element parameterizations are employed: SEP1+NSED (left panels) and SEP2+SED2 (right panels). The relative errors are computed using Eq. 45 and replacing DeltaVAF by the grounding line position.

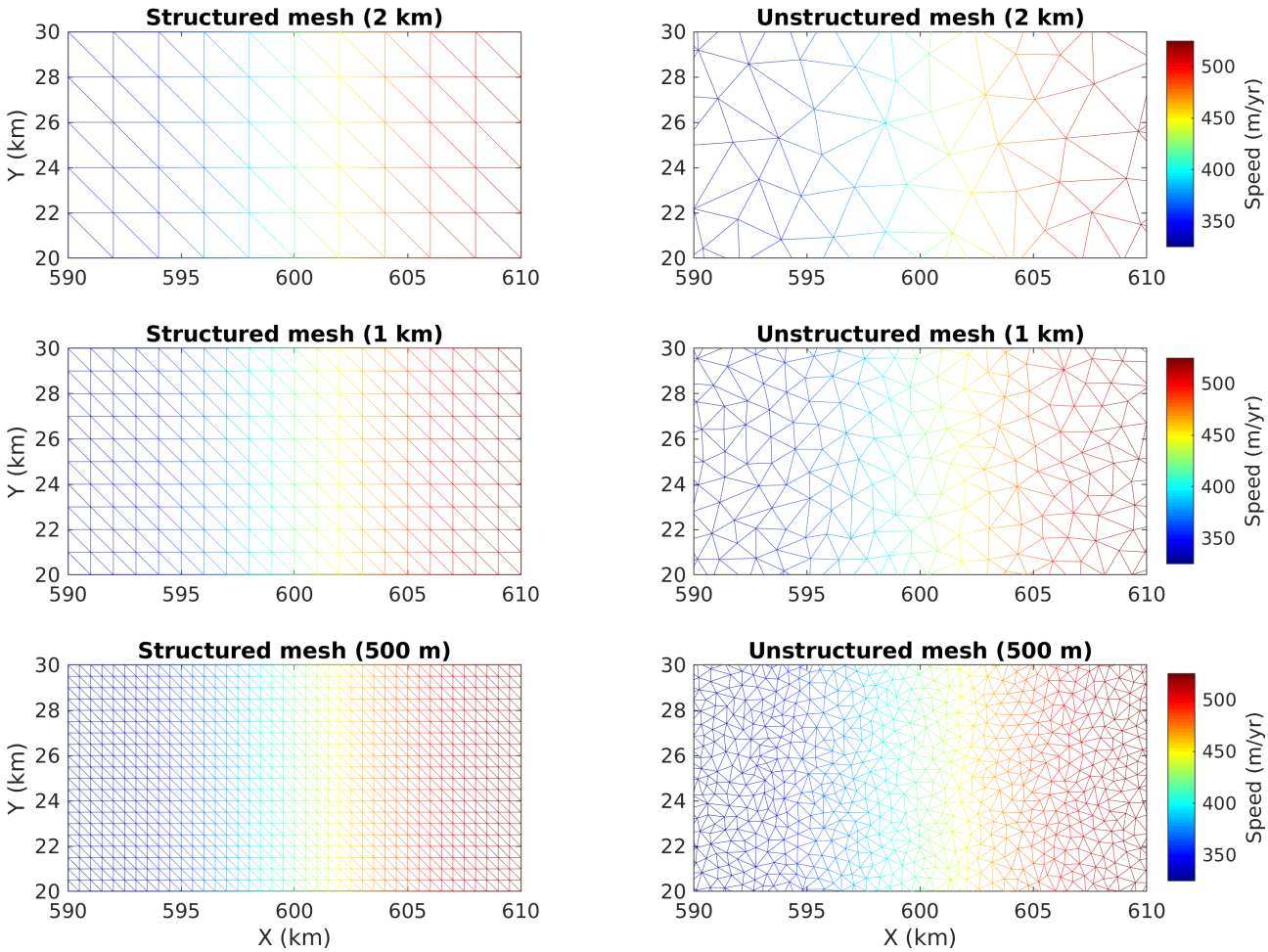

Figure B1. Examples of meshes employed in this work. Left panels are structured conforming meshes, and right panels the unstructured meshes. Three mesh resolutions are shown: 2, 1, and 0.5 km. The colormaps are the ice speeds obtained in the diagnostic analysis (Sec. 5,1) considering the grounding line at x=600 km. Note that the structured meshes are conforming to the grounding line, i.e., they are generated such that the elements' edges match the grounding line position (in this case, xgl=600 km). Sub-element parameterizations SEP1+NSED are employed in the unstructured meshes to computed the ice speeds presented here.